Using Nature's polyenes as templates: Studies of synthetic xanthomonadin analogues and realising their potential as antioxidants

Katrina S. Madden,[a] Hans R. E. Jokhoo,[b] Fabian D. Conradi,[b] Jonathan P. Knowles,[c],[d] Conrad W. Mullineaux[b]* and Andrew Whiting[a]*

[a] Department of Chemistry, Durham University, Science Site, South Road, Durham, DH1 3LE, UK. Email: andy.whiting@durham.ac.uk

[b] School of Biological Sciences, Queen Mary University of London, Mile End Road, London, E1 4NS. Email: c.mullineaux@qmul.ac.uk

[c] Department of Applied Sciences, Northumbria University, Northumberland Building, College Lane, Newcastle, NE1 8SG, UK

[d] Department of Chemistry, University of Bristol, Cantock's Close, Bristol, Avon, BS8 1TS, UK.

Supporting information for this article is given via a link at the end of the document.

Graphical abstract

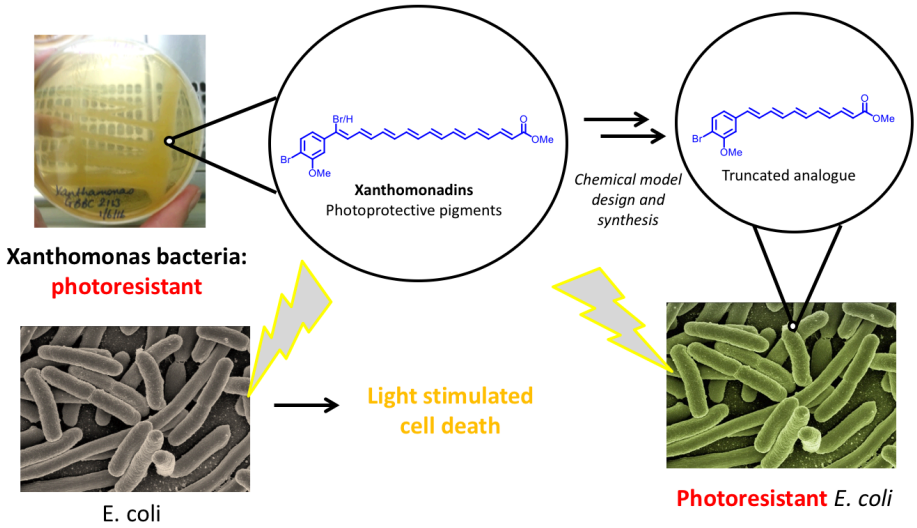

Two truncated analogues of the polyenyl photoprotective xanthomonadin pigments have been synthesised utilising an iterative Heck-Mizoroki (HM)/iododeboronation cross coupling approach and investigated as models of the natural product photoprotective agents in bacteria. Despite the instability of these types of compounds, both analogues proved to be sufficiently stable to allow isolation, spectroscopic analysis and biological studies into their photoprotective behaviour which showed that despite their shorter polyene chain

length, they retained the ability to protect bacteria from photochemical damage; i.e. incorporation of one compound into *E. coli* provided photoprotective activity against singlet oxygen analogous to the natural photoprotective mechanisms employed by *Xanthomonas* bacteria, answering key questions about what minimal functionality is required to impart photoprotection, potentially leading to new classes of photoprotective and antioxidants compounds.

Introduction

Members of the bacterial genus *Xanthomonas* are the cause of a number of plant diseases e.g. *Xanthomonas oryzae pv. oryzae* (rice blight) and *Xanthomonas campestris pv. campestris* (black rot of crucifers) and these bacteria form characteristic yellow colonies due to the yellow, weakly fluorescent, membrane-bound pigments they produce (Figure 1).[1-12] The presence of these types of pigments in the cell membranes is key to the survival of these types of bacteria on leaf surfaces that are exposed to potentially high levels of UV light. Indeed, Starr *et al*. structurally identified these pigments and hence, recognised the *Xanthomonas* pigments' similarity to the carotenoids. As a result, they postulated that their biological role may be to protect the bacteria from photodamage. Indeed, xanthomonadin **1** (isolated from the bacteria) was shown to protect *Xanthomonas juglandis* strain XJ103 from photodamage, but whether or not the pigment protected the bacterium from oxygen-related killing was not determined.[13] The Sonti group showed that xanthomonadin did indeed display antioxidant properties in *Xanthomonas oryzae pv. oryzae* in 1997[12] and that it protected membrane lipids from peroxidation. The mechanism of this bacterial survival has been investigated by the Poplawsky *et al.* in the Xanthomonas genus[2–11] and in 2000, the role of xanthomonadin in *Xanthomonas campestris pv. campestris* was reported. It was concluded that it is unlikely that the xanthomonadin pigments offer protection against direct UV damage, rather they likely offer protection when a photosensitiser was present. They also showed that a diffusible factor was needed for xanthomonadin production *via* quorum sensing and that the pigB transcriptional unit was vital for bacterial survival. [2,6]

A number of other related pigments made by different bacteria have also been partially identified, or rather proposed in the literature.[14–16] The main characteristics of these types of systems (Figure 1) being a long polyene chain of varying length (commonly an octaene) flanked by an ester group at one end, a substituted phenyl group at the other and the entire natural product being somewhat unstable in air and light. Studies of these pigments have provided an insight into the biosynthesis of the xanthomonadins, in particular the installation of the bromines on the scaffold. The pigment made by *Lysobacter enzymogenes* is non-brominated and the bacterium does not possess a halogenase enzyme, suggesting that such enzymes are likely key to the installation of bromide functionalities.[14] In fact, the presence of bromide functions in such molecular systems is interesting from a chemical, photophysical and mode of action standpoint. Presumably, following initial formation of a singlet excited state upon UV irradiation, the presence of a bromine atom(s) in xanthomonadin-type systems would be expected to lead to a large increase in the rate of spin-forbidden intersystem crossing (ISC) to the triplet form by means of interaction with the bromine atom's large orbital

angular momentum; the so-called heavy atom effect.[17] This process could offer considerable advantages in a molecule whose function is as a photoprotective agent. Most notably, singlet-singlet excitation processes have previously been shown to operate upon irradiation of carotenoids[18] and this has the potential to lead to damaging photosensitised reactions within bacterial cells. Rapid conversion from singlet to triplet excited states in order to avoid this could therefore be beneficial. Additionally, the presence of a heavy atom is known to decrease the lifetime of the triplet states formed in such pathways,[19,20] resulting in the further reduction of the risk of unwanted triplet-triplet photosensitised reactions and leading to an increased rate of regeneration of the photoprotective agent. Hence, probing such systems and models thereof, has potential repercussions for understanding and in future, designing photoprotective systems.

Xanthomonadin pigments are also of potential interest for a number of other reasons beyond immediate structure-activity aspect as bacterial photoprotective systems, raising a number of intriguing questions, including understanding why such long chain polyenes are made by these bacteria when perhaps, simpler, more stable photoprotective compounds could be accessible. Additionally, and perhaps more importantly, it is necessary to understand the survival mechanisms of such virulent plant pathogens, and there is an increasing body of evidence suggesting a role of antioxidants in combatting disease. This could therefore lead to possible applications in neurodegenerative and inflammatory diseases such as atherosclerosis, and in cancer (amongst others[21-23]), demonstrating a clear benefit of understanding the functionality behind the photoprotective ability of this class of compounds. Ultimately this understanding could perhaps be used as a design template from which to harness their reactivity though the synthesis of more accessible analogues, generating potentially novel types of antioxidants and photoprotective agents in general.

Figure 1 Images of *Xanthomonas* sp. GBBC2252 and the structure of isolated xanthomonadin pigment **1** with the characterisation data obtained by Andrewes *et al.*[13,24,25] (image bottom left is a confocal fluorescence micrograph showing xanthomonadin fluorescence at the cell envelope).

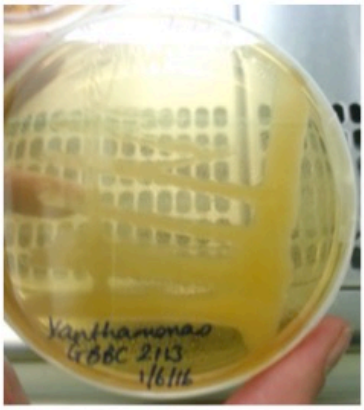

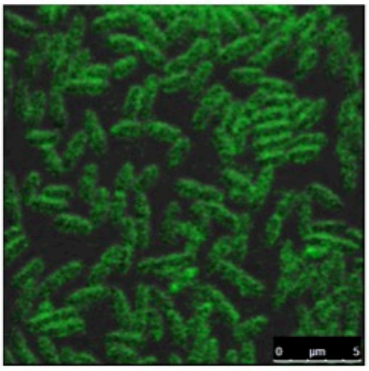

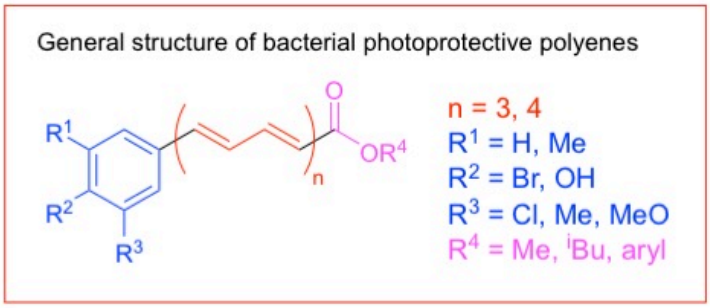

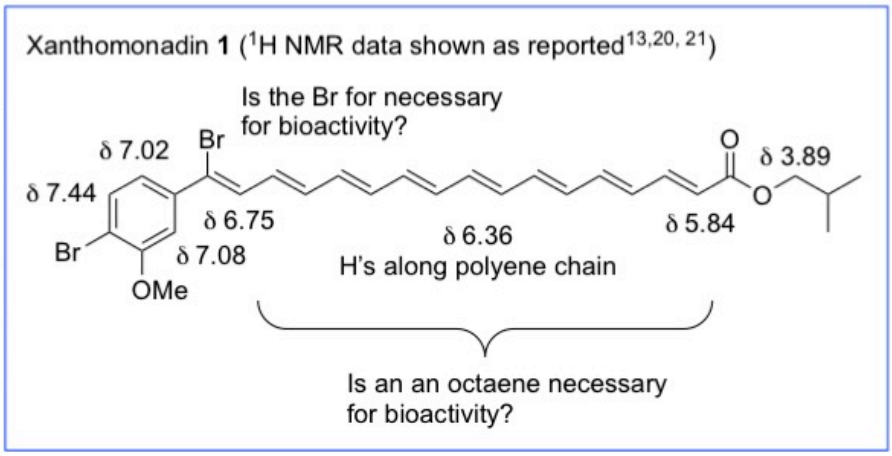

One of the key challenges for any synthesis and investigation of the xanthomonadin pigments is the lack of complete, high quality, spectroscopic characterisation. This lack of completely convincing structural information, as well as a lack of stability studies, means that in most cases synthetic, stability and biological studies are required.[22] Interestingly, one of the few systems mostly characterised to a reasonable extent (though some years ago now) is xanthomonadin **1**, with some reported low resolution ^{1}H NMR data, along with ESI and UV-Vis data (see Figure 1).[13,24,25] Evidence for a debrominated xanthomonadin methyl ester analogue **2b** was also obtained, but only in the form of mass spectrometry and UV-Vis spectroscopy.[13,24] The lack of stability and basic structural information suggests a potential synthetic challenge and goal, and hence, coupled with their role as photoprotective agents, makes these systems intriguing synthetic targets as they stand, but also, a possible basis for the design of novel photoprotective/antioxidants species. Hence, studies were undertaken to understand why polyenic systems typified by xanthomonadins of general type **1** have not been prepared to date, why Nature might want to make such seemingly unnecessarily complex and long polyenic systems to use as antioxidants, and therefore, whether one could simplify the design and still retain antioxidant properties. In this paper, we report synthetic studies working towards analogues of xanthomonadin **2**, through the synthesis of simpler, shorter systems that are sufficiently stable and retain the photoprotective properties of the natural system.

Results and discussion

Synthesis of truncated model xanthomonadin analogues

Our envisaged disconnection of xanthomonadins such as **2**[26] involved utilising the flexibility of our Heck-Mizoroki/iododeboronation (HM/IDB) methodology as an iterative process by which to efficiently construct polyenyl intermediates. The key strategic aim was to assemble building blocks of whichever length imparts the greatest stability and assemble these using palladium cross-coupling chemistry, i.e. as outlined in Scheme 1a.[27–31] Having already established routes to key styrenyl building blocks and performed preliminary investigations into their cross-coupling,[26] we decided to focus on the synthesis of two truncated model compounds. These shorter systems would enable us to test out both final cross-coupling conditions on systems more like the final natural product pigments, and to probe the functionalities and polyene chain length required to impart photoprotective activity. In designing these new synthetic target analogues (Scheme 1), we aimed to better understand the minimal polyene chain necessary for imparting photoprotective biological activity, since the reported pigments contain mostly octaenes, with some heptaenes and hexaenes, but literature searches did not reveal any shorter polyene chain length systems. As a result, we aimed to synthesise pentaenyl models without the bromine substituent on the polyene component, with a view to ascertaining their photoprotective potential. Therefore, we designed two models systems: pentaene **13**, a debrominated shorter analogue of the xanthomonadin system, and tetraeneyne **12**, with an alkyne next to the aryl group and a tetraenyl chain conjugated to the ester function (see Scheme 1b). Access to systems **12** and **13** could be envisaged by starting with styrenyl building blocks and vinyl iodide **7** (*i.e.* as previously reported[26,32]).

Scheme 1 a) Retrosynthetic strategy for xanthomonadin pigments **2** synthesis; b) Proposed synthesis of xanthomonadin analogues **12** and **13**.

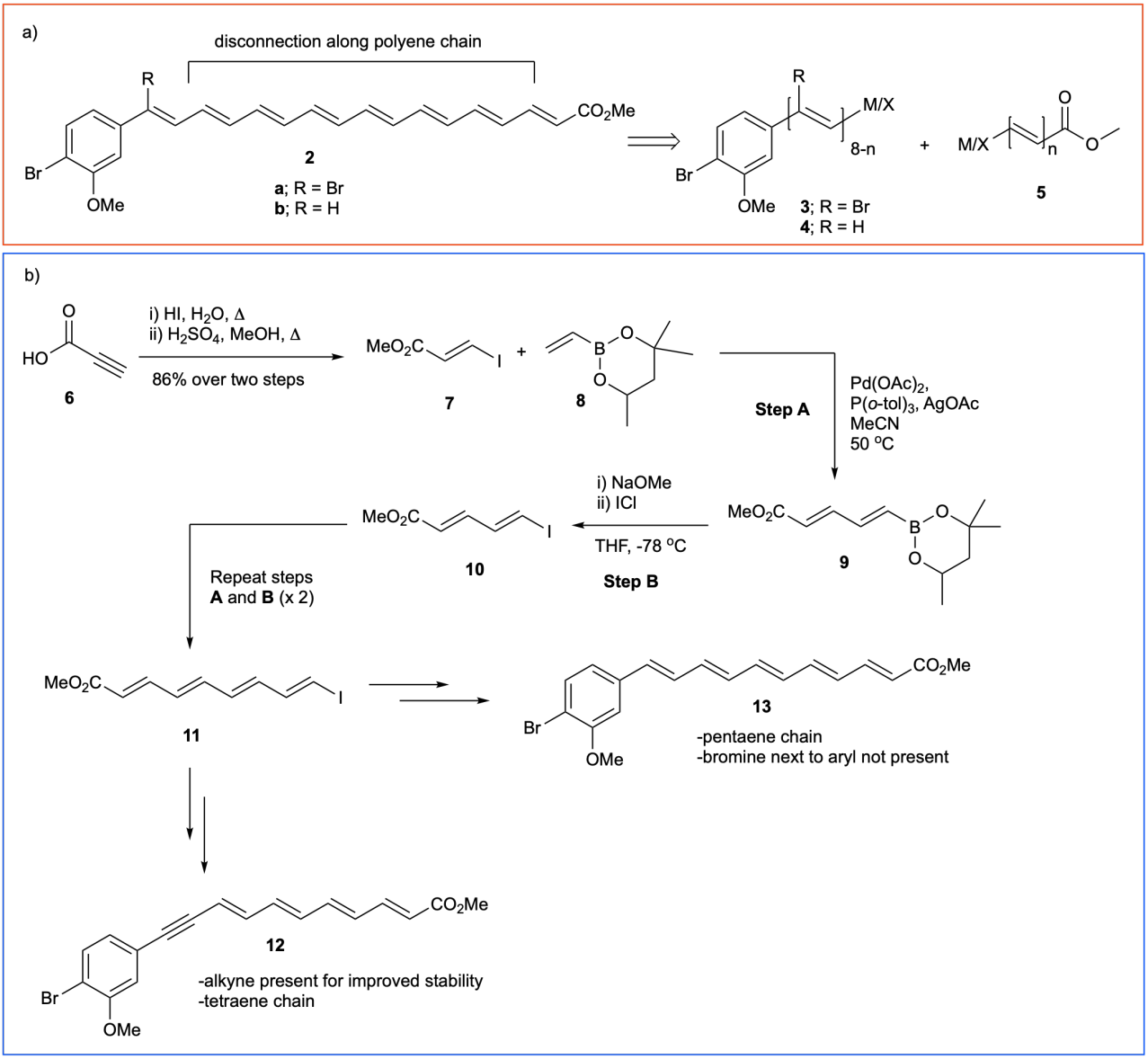

Following this synthetic plan (Scheme 1), HM/IDB methodology was indeed successfully utilised to furnish the key tetraenyl intermediate **11**, in 20% overall yield (average of 76% per step over 6 steps (see Scheme 2). Whilst tetraene **11** was unstable in air and light, this intermediate could be stored under argon at -18 °C for up to two months.

Scheme 2 Syntheses of truncated model xanthomonadin analogues **12** and **13**

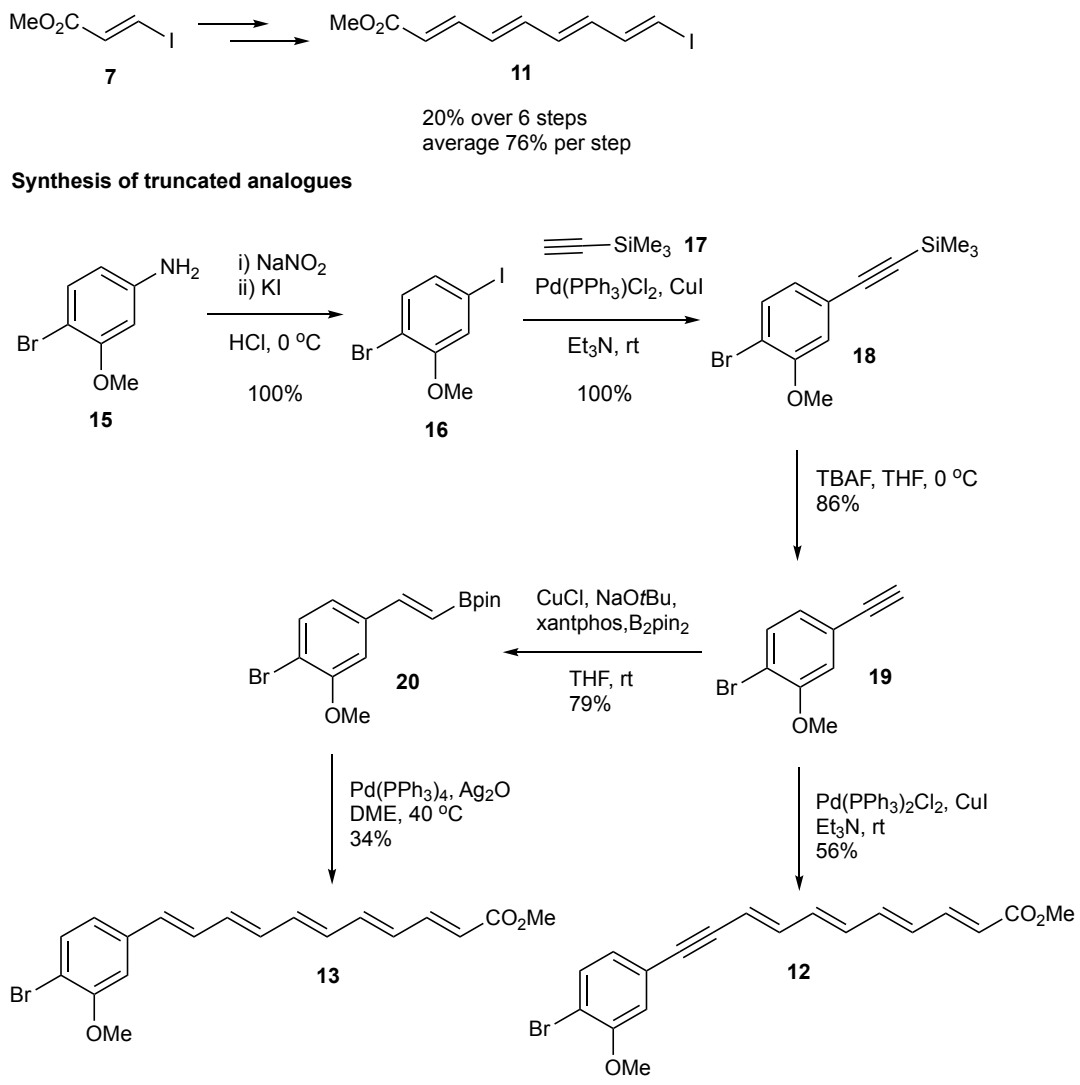

Styrenyl building blocks **19** and **20** were synthesised as reported elsewhere,[26] *via* Sonogshira and Suzuki-Miyaura cross-couplings to give the desired target compounds **12** and **13**. Whilst both final couplings (Figure 3) to derive compounds **12** and **13** proceeded with high conversion, final isolation and therefore isolated yields were moderate due to the instability of the final products on silica gel, highlighting the inherent instability of even shorter chain analogues. Nevertheless, pentaenyl analogue **13** was successfully obtained by Suzuki-Miyaura cross-coupling of tetraenyl iodide **7** with styrenyl building block **20** in a 34% yield, and alkynyl tetraenyl analogue **12** by Sonogashira cross-coupling from styrenyl building block **19** in a 56% yield (Scheme 2). Other analytical data, especially NMR data, for truncated model xanthomonadin analogues **12** and **13** was consistent with those reported for xanthomonadin **1**, as highlighted in Table 1. ^{1}H NMR data for analogues **12** and **13** shows a good correlation with the NMR data reported for xanthomonadin **1** (see Figure

1). The spectra for both these analogues **12** and **13** shows additional peaks with smaller alkene couplings, suggesting a small proportion of *cis-trans (E-Z)* isomerism in one of the double bonds (see Tables 1a and 1b); a proposal which has evidence from UV-Vis spectroscopy (*vide infra*).

Table 1 detailing: 1a) ^{1}H NMR data for xanthomonadin model **12**; 1b) ^{1}H NMR data for xanthomonadin model **13**; 3) UV-Vis and fluorescence data for xanthomonadin **1** and models **12** and **13**.

Table 1a ^{1}H NMR data for analogue **12**			**Table 1b** ^{1}H NMR data for analogue **13**	
Entry	Dehydro-tetraen-yne analogue **12** δ_H	Minor component (~5%), new identifiable signals δ_H	Pentaene analogue **13** δ_H	Minor component (11%) δ_H
1	5.89 (1H, d, *J* 15.2 Hz)	5.74 (1H, d, *J* 10.5 Hz)	5.91 (2H, dd, *J* 15.3, 6.1 Hz)	5.72 (1H, d, *J* 11.2 Hz)
2	6.37 (2H, dd, *J* 14.7, 11.2 Hz)	7.64 (1H, d, *J* 8.1 Hz)	6.29-6.54 (3H, m)	5.74-5.79 (1H, m)
3	6.41-6.52 (3H, m)	7.74 (1H, d, *J* 7.9 Hz)	6.60 (1H, dd, *J* 14.8, 10.5 Hz)	6.21 (1H, t, *J* 11.5 Hz)
4	6.55 (1H, d, *J* 15.5 Hz)		6.75 (1H, dd, *J* 15.4, 10.4 Hz)	7.78 (1H, d, *J* 12.4 Hz)
5	6.62 (1H, dd, *J* 14.7, 11.2 Hz)		6.89-6.99 (2H, m)	7.82 (1H, d, *J* 12.0 Hz)
6	6.80-6.85 (1H, m)		7.28-7.39 (1H, m)	
7	6.87-6.93 (2H, m)		7.49 (1H, dd, *J* 11.4, 8.3 Hz)	

Table 2 UV-Vis and fluorescence data for xanthomonadin **1** and models **12** and **13**, along with calculated λ_{max} values

Entry	Compound	UV-Vis absorption/nm	λ_{max} (calc.)/nm	Emission/nm
1	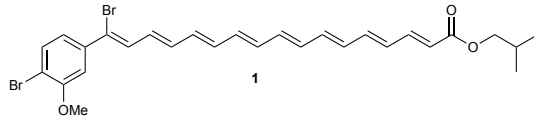 **1**	453, 482 ($CHCl_3$)	459 (489[a])	-
2	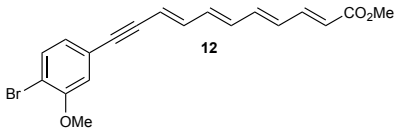 **12**	397, 417 ($CHCl_3$)	417	498, 527, 566, 594
3	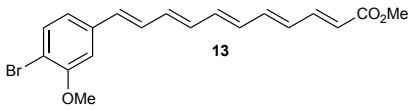 **13**	370, 391 (Et_2O)	392	440, 468, 494

[a]Effect of adding a 30 nm contribution for a bromine function attached to the polyene in the ✔-aryl position.

Equation 1 $\lambda_{max} = 114 + 5M + n(48.0 - 1.7n) - 16.5R_{endo} - 10R_{exo}$

Where: n = the number of conjugated double bonds; *M* = the number of alkyl or alkyl-like substituents; R_{endo} = the number of rings with *endo*cyclic double bonds; R_{exo} = the number of rings with *exo*cyclic double bonds

Key findings from comparing of the spectral data in Tables 1a and 1b for compounds **12** and **13** with that of xanthomonadin **1** are: 1) That the absorption maxima for analogues **12** and **13** are lower than those of **1**, consistent with the shorter conjugated polyene chain; 2) That the decrease in absorption maximum is greater for yne-tetraene **12** than for pentaene **13**, suggesting a longer effective conjugated length in the pentaene (*vide infra*); 3) That application of Fieser-Kuhn rules[33] (Equation 1), which were developed for related carotenoids, provide a reasonable comparison for the absorptions estimated for xanthomonadin **1** (note that

the bromine substituent on the polyene can be expected to add *ca*. 30 nm to the calculated λ_{max}[34]) *versus* the two analogues. Indeed, the calculated λ_{max} values for **12** and **13** correspond well with the lowest energy λ_{max} observed; 4) That the minor, higher energy (*i.e.* shorter wavelength) peaks are consistent with some *trans*- to *cis*-isomerisation. Such a phenomenon is well established (e.g. *trans*- to *cis*-stilbene interconversion gives two λ_{max}'s of 307 and 276 nm, respectively[35]) and in systems herein it appears likely that the lower absorptions (453 for xanthomonadin, 397 for **12**, and 370 for **13** (Table 2) are due to the minor *cis*-isomer being present in equilibrium, and indeed, this is further supported by ^{1}H NMR data which is consistent with the isomerised alkene being the γ,δ-double bond relative to the ester carbonyl; 5) The most accurate calculation of λ_{max} for yne-tetraene **12** comes from assuming that the alkyne allows conjugation to continue throughout the molecule but does not increase the conjugated length in itself (411 nm being obtained if it is counted as an additional alkene unit), which is a potentially important consideration when using such functional groups in the synthesis of stable polyene analogues.

Exposure of *E. coli* cells with truncated xanthomonadin analogues 12 **and** 13

Xanthomonadin **1** is weakly fluorescent, allowing the location and relative concentration of xanthomonadin **1** to be probed *in vivo* by fluorescence microscopy. We recorded confocal fluorescence images of four wild-type *Xanthomonas* strains using excitation and emission wavelengths appropriate for xanthomonadin **1** (Figure 2). *Xanthomonas arboricola* GBBC2191 has larger cells than the other strains and showed relatively strong xanthomonadin **1** fluorescence (Figure 2a). The remaining three strains that we examined all have smaller cells and showed weak, but detectable, fluorescence from the cell surface layers, as exemplified by *Xanthomonas* sp. GBBC2252 (Figure 2b-d). Unlabelled *E. coli* cells showed no detectable fluorescence when imaged with the same settings (Figure 2g). However, exposure (i.e. staining) to pentaenyl analogue **13**, followed by washing off, the *E. coli* cells showed a fluorescence signal that was just a little lower than that seen in *Xanthomonas* sp. GBBC2252, although considerably less than that seen in *Xanthomonas arboricola* (Figure 2e-f). This showed that compound **13** was readily taken up into the these cells, and was incorporated into all the *E. coli* cells in the suspension (Figure 2f). Doubling the concentration of analogue **13** did not noticeably increase the labelling of the *E. coli* cells (not shown). Indeed, the resulting images in Figure 2 suggest that incubation with analogue **13** solution results in incorporation of **13** into the *E. coli* membranes at levels comparable to the native levels in some *Xanthomonas* species. By contrast, a similar incubation with alkynyl tetraenyl analogue **12** solution did not result in any detectable incorporation into *E. coli* cells, although fluorescence was observed in small crystals or aggregates close to the cells (Figure 2h). It appears that analogue **12** may not be bioavailable as a result of crystallisation under the conditions of the exposure of the *E. coli* experiment.

Figure 2 Xanthomonadin fluorescence from *Xanthomonas* species and *E. coli* loaded with compounds **12** or **13** (scale-bars 5 µm): a. Fluorescence image of *Xanthomonas arboricola* GBBC2191; b. Fluorescence image of *Xanthomonas* sp. GBBC2252 [same intensity scale as (a) for comparison]; c. Fluorescence image of *Xanthomonas* sp. GBBC2252 [intensity-scale enhanced by a factor of 8 compared to (a) and (b)]; d. Merged bright-field and fluorescence image of *Xanthomonas* sp. GBBC2252; e. Fluorescence image of *E. coli* cells loaded with exogenous **13** [same intensity scale as (c)]; f. Merged bright-field and fluorescence image of *E. coli* cells loaded with exogenous **13**; g. Merged bright-field and fluorescence image of unlabelled *E. coli* cells [same intensity scale as (f)]; h. Merged bright-field and fluorescence image of *E. coli* cells loaded with exogenous **12** [same intensity scale as (g)].

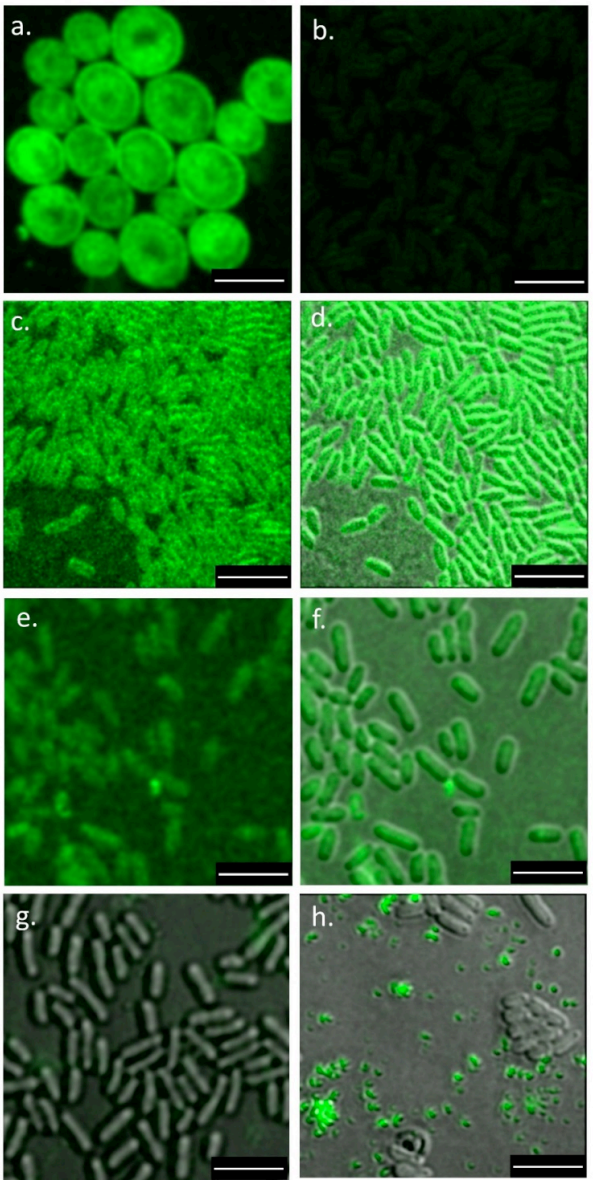

Table 3 Effect of pre-incubation with compounds **12** and **13** on the survival rates of *E. coli* cells following exposure to light in the presence of Rose Bengal (*n* = number of replicate experiments). Each experiment involved counting plates which contained *ca.* 50-100 colonies when untreated cells were plated out. Control: cells without addition of a xanthomonadin analogue, Survival rates are relative to cells not exposed to Rose Bengal and light.

Treatment	Mean survival rate ± SD	T-test (vs control)
Control	0.56 ± 0.13 (*n* = 6)	
12	0.37 ± 0.25 (*n* = 3)	*p* = 0.15
13	0.95 ± 0.06 (*n* = 3)	*p* = 0.002

Truncated xanthomonadin analogue 12 **confers photoprotection to *E. coli***

To test whether incorporation of analogues **12** and **13** into *E. coli* cells confers protection against reactive oxygen species (ROS), we measured cell survival rates following a treatment with Rose Bengal, which is a potent source of singlet oxygen when illuminated. Treatments with Rose Bengal in the dark, or with light in the absence of Rose Bengal, had no significant effect on cell survival (not shown). However, treatment with light in the presence of Rose Bengal killed nearly half the cells under our conditions, as judged from colony counts (Table 3). Remarkably, pre-incubation with pentaenyl analogue **13** conferred essentially complete protection against the ROS treatment, with no significant cell death observed. However, alkynyl tetraenyl analogue **12** conferred no protection against the ROS treatment (Table 3).

Pentaenyl analogue **13** can also be added exogenously to *E. coli* and is incorporated into the cell at levels comparable to those found in *Xanthomonas* species (Fig. 2). Incorporation of **13** in this way into *E. coli* confers strong protection against ROS, providing a direct demonstration of the efficacy of **13** as a ROS quencher in a biological context. Alkynyl tetraenyl model **12** was not detectably incorporated into *E. coli* cells following a similar incubation to that used for **13** and this lack of bioavailability is likely due the observed formation of crystalline aggregates that could well prevent take up of this particular compound, unlike the more bioavailable compound **13** (Fig. 2). From that perspective, it would not be surprising that model **12** did not confer any significant protection against ROS, because it was not sufficiently bioavailable in the culture conditions used. This reinforces the fact that the xanthomonadin (or synthetic analogue) has to be actually be incorporated into the cell to confer protection, *i.e.* just quenching ROS in the surrounding medium is not sufficient.

Conclusions

Truncated models of xanthomonadin pigments **1** and **2** were successfully synthesised and their photoprotective activity analysed in *E. coli*. The spectroscopic data obtained supports the characterisation previously obtained for xanthomonadin, and is consistent with the shorter chain length of these molecules. Pentaenyl analogue **13** was observed to be incorporated into the cell membrane and able to impart photoprotective activity analogous to that of the natural product. Alkynyl tetraenyl analogue **12**, however, was not incorporated, forming crystalline aggregates outside of the cells, and did not impart increased protection of *E. coli*. The activity of debrominated pentaenyl analogue **13** shows that the presence of the bromine located on the polyene system in xanthomonadin **1** is not necessary for activity, and more importantly, it also shows that a pentaene is sufficient to impart photoprotection. This observation leaves us to hypothesise that the role of the bromine might be to impart stability to the polyene chain and to tune photoactivity through increase intersystem crossing through the heavy atom effect (*vide supra*), rather than being absolutely necessary for activity.

Pentaenyl analogue **13** has been shown to be a suitable truncated model for the xanthomonadin pigment class of compounds, which should allow for the further study of the photoprotective abilities of this interesting

family of plant pathogens. Further studies applying this type of methodology is likely to enable the test for protection against ROS conferred by other synthetic variants of the xanthomonadins in more detail and to establish whether the antioxidant properties of this class of compounds can be utilised in other therapeutic contexts, including as novel antioxidants.

Conflicts of interest

There are no conflicts to declare.

Acknowledgements

We would like to thank the EPSRC for the award of a Doctoral Training Grant to K. S. M.

Notes and references

1 Y. Shen and P. Ronald, *Microbes Infect.*, 2002, **4**, 1361–1367.
2 A. R. Poplawsky, S. C. Urban and W. Chun, *Appl.Environ.Microbiol.*, 2000, **66**, 5123–5127.
3 A. R. Poplawsky, M. D. Kawalek and N. W. Schaad, *Mol. Plant-Microbe Interact.*, 1993, **6**, 545–545.
4 W. Chun, J. Cui, and A. R. Poplawsky, *Physiol. Mol. Plant Pathol.*, 1997, **51**, 1–14.
5 A. R. Poplawsky and W. Chun, *J. Bacteriol.*, 1997, **179**, 439–444.
6 A. R. Poplawsky and Chun, *Mol. Plant-Microbe Interact.*, 1998, **11**, 466–475.
7 A. R. Poplawsky, W. Chun, H. Slater, M. J. Daniels and J. M. Dow, *Mol. Plant-Microbe Interact.,* 1998, **11**, 68–70.
8 A. R. Poplawsky, D. M. Walters, P. E. Rouviere and W. Chun, *Mol. Plant Pathol.,* 2005, **6**, 653–657.
9 A. Yajima, N. Imai, A. R. Poplawsky, T. Nukada and G. Yabuta, *Tetrahedron Lett.,* 2010, **51**, 2074–2077.
10 L. Zhou, J. Y. Wang, J. Wu, J. Wang, A. R. Poplawsky, S. Lin, B. Zhu, C. Chang, T. Zhou, L. H. Zhang, and Y. W. He, *Mol. Microbiol.*, 2013, **87**, 80–93.
11 L. Zhou, T. W. Huang, J. Y. Wang, S. Sun, G. Chen, A. R. Poplawsky and Y. W. He, *Mol. Plant. Microbe. Interact.,* 2013, **26**, 1239–48.
12 L. Rajagopal, C. S. S. Sundari, D. Balasubramanian and R. V. Sonti, *FEBS Lett.,* 1997, **415**, 125–128.
13 M. P. Starr, C. L. Jenkins, L. B. Bussey and A. G. Andrewes, *Arch. Microbiol.*, 1977, **113,** 1–9.
14 T. A. Schöner, S. W. Fuchs, B. Reinhold-Hurek and H. B. Bode, *PLoS One,* 2014, **9**, e90922.
15 P. Cimermancic, M. H. Medema, J. Claesen, K. Kurita, L. C. Wieland Brown, K. Mavrommatis, A. Pati, P. A. Godfrey, M. Koehrsen, J. Clardy, B. W. Birren, E. Takano, A. Sali, R. G. Linington, and M. A. Fischbach, *Cell,* 2014, **158**, 412–421.
16 C. L. Jenkins and M. P. Starr, *Curr. Microbiol.,* 1982, **7**, 323–326.
17 N. J. Turro, Modern molecular photochemistry, University Science Books, Mill Valley, CA., 1991.
18 R. Bensasson, E. A. Dawe, D. A. Long andE. J. Land, *J. Chem. Soc, Faraday Trans. I*, 1977, **73**, 1319-1325.
19 Z. S. Romanova, K. Deshayes and P. Piotrowiak, *J. Am. Chem. Soc*., 2001, **123**, 2444-2445.
20 G. Kavarnos, T. Cole, P. Scribe, J. C. Dalton, and N. J. Turro, *J. Am. Chem. Soc.*, 1971, **93**, 1032-1034.
21 J. D. Hayes, S. A. Chanas, C. J. Henderson, M. McMahon, C. Sun, G. J. Moffat, C. Wolf and M. Yamamoto, *Biochem. Soc. Trans.*, 2000, **28**, 33–41.
22 L. Luliano, A. R. Colavita, C. Camastra, V. Bello, C. Quintarelli, M. Alessandroni, F. Piovella, and F. Violi, *J. Pharmacol.*, 1996, **119**, 1438–1446.
23 A. Augustyniak, G. Bartosz, A. Cipak, G. Duburs, L. Horáková, W. Luczaj, M. Majekova, A. D. Odysseos, L. Rackova, E. Skrzydlewska, M. Stefek, M. Strosová, G. Tirzitis, P. R. Venskutonis, J. Viskupicova, P. S. Vraka and N. Zarković, *Free Radic. Res.*, 2010, **44**, 1216–1262.

24 A. G. Andrewes, S. Hertzberg, S. Liaaen-Jensen and M. P. Starr, *Acta Chem. Scand.*, 1973, **27**, 2383–95.
25 A. G. Andrewes, C. L. Jenkins, M. P. Starr, J. Shepherd and H. Hope, *Tetrahedron Lett.*, 1976, **45**, 4023–4024.
26 K. S. Madden, B. Laroche, S. David, A. S. Batsanov, D. Thompson, J. P. Knowles and A. Whiting, *Eur. J. Org. Chem.*, 2018, 38, 5312-5322.
27 S. K. Stewart and A. Whiting, *Tetrahedron Lett.*, 1995, **36**, 3925–3928.
28 S. K. Stewart and A. Whiting, *Tetrahedron Lett.*, 1995, **36**, 3929–3932.
29 N. Henaff and A. Whiting, *Org. Lett.*, 1999, **1**, 1137–1139.
30 J. P. Knowles, V. E. O′Connor and A. Whiting, *Org. Biomol. Chem.*, 2011, **9**, 1876-1886.
31 K. S. Madden, S. David, J. P. Knowles and A. Whiting, *Chem. Commun.*, 2015, **51**, 11409–11412.
32 J. P. Knowles, V. E. O′Connor and A. Whiting, *Org. Biomol. Chem.*, 2011, **9**, 1876 (2011).
33 S. Kumar, *Specorganic*, 2006, 51–67.
34 L. Dorfman, *Chem. Rev*., 1953, **53**, 47-144.
35 J. G. Grasselli and W. M. Ritchey, Atlas of spectral data and physical constants for organic compounds, 2nd. Edn., CRC press, Cleveland, USA, 1975.